International Journal of Engineering

Effect of Mechanical Alloying and Sintering on Phase Transformation, Microstructural Evolution, Mechanical Properties and Density of Zr-Cr Alloy

J. Arasteh*

Department of Materials Science and Engineering, Shahid Bahonar University of Kerman, Kerman, Iran

PAPER INFO	ABSTRACT
	The purpose of present research was production of Zr-based alloy as the nuclear fuel cladding by mechanical alloying (MA) and sintering process. Firstly, Zr and Cr powders were mechanically alloyed to produce the refractory and hard Zr-10 wt% Cr alloy, and then, the powder mixtures were consolidated by press and following sintering at temperature of 800˚C min. The phase evolution, microstructural changes, microhardness, and density of the Zr-10 wt% Cr alloy were studied using X-ray diffraction (XRD), scanning electron microscopy (SEM), microhardness measurement, and the Archimedes method. The results showed that the MA increased the solid solubility of the immiscible powders of Cr and Zr; therefore, the Cr atoms were completely dissolved in the Zr lattice after 24 h of the milling time and the nanostructured Zr(Cr) solid solution was obtained with the high microhardness value of about 491 Hv. Also, the results of the density measurement indicated that the resulted density was close to 98% of the theoretical density.

1. INTRODUCTION

Zirconium alloys are considered as a high temperature structural materials owing to proper corrosion resistance, good thermal stability, desired mechanical and physical properties, and low thermal neutron absorption properties [1]. Cr is a useful alloying element for Zr-based alloys owing to high melting point, and also, Zr-Cr alloys can be used as a high temperature material with good strength, proper erosion resistance, and excellent corrosion resistance. So far, extensive research has been done on Zr-Cr alloys. The microstructural examination of the rapidly cooled Zr-0.15% Cr alloy showed that a Zr-rich solid solution was formed. This solid solution phase was precipitated in the grain boundaries of Zr which increased the microhardness and strength of the Zr-Cr alloy [2]. The Zr-Cr multilayer coating on Zr surface by vacuum arc vapor method was significantly increased the hot corrosion resistance of the Zr-based alloy [3]. The Cr

ion implantation was subjected on the Zr-1Nb alloy to improve the corrosion behavior of Zr-based alloy, which the result showed the laves phase was homogeneously precipitated within the α-Zr matrix. Also, the oxidation resistance of the Zr-based alloy was improved at high temperature due to the Cr ion implantation on the surface of Zr [4]. Huang et al. [5] have produced Cr coated Zr-based alloy by electroplating which the result indicated that the oxidation resistance of Zr-based alloy cladding was significantly improved. Also, pulsed laser treatment was subjected to the commercial Zr alloy to perform the Cr alloying on the Zr surface. The results of this research displayed that the microhardness of Zr was noticeably increased due to the microstructure improvement and grain refinement [6].

So far, many methods have been used to produce the Zr-Cr alloys, but the mechanical alloying method has always attracted the attention of the researchers due to the low cost of the instrument and primary powders [7], production of the stable and metastable phases [8, 9] no need for high temperatures [10], alloying of the elements with high difference in the melting points [11], independency of the limitation of the phase diagram

*Corresponding Author Email: *javadaraste68@gmail.com* (J. Arasteh)*

[12], ability to the uniform distribution of the components, and production of the nanostructure materials and quasi-stable microstructures [13-14]. The mechanical alloying accelerated the kinetic of the chemical reactions and changed the metallurgical transformations which led to occur the reactions at room temperature [15]. Researchers have proven that chromium is a very suitable additive element to improve the mechanical properties [16] and corrosion resistance [17] of Zr which indicates that the Zr-Cr alloys have the special importance among the Zr-based alloys. But in the Zr-Cr alloy system, the solid solubility of Cr in Zr is very low at the equilibrium state [18]. The solubility of these elements can be increased by nonequilibrium processes such as mechanical alloying. The purpose of this research was to produce a solid solution of Zr-Cr alloy with high hardness by mechanical alloying and sintering process. Also, the phase evolution, structural and morphological changes, mechanical properties, and physical properties of the Zr-Cr alloys were investigated.

2. MATERIALS AND METHODS

In the present research, planetary ball mill (84 D, Sepahan) was used to produce Zr- 10% Cr alloy. Therefore, the Cr and Zr powders (99.9% purity, prepared by Alpha Aesar) were firstly mixed according to the weight ratio of Zr-10 wt% Cr. Then, 10 g powder mixtures of Cr and Zr along with the 200 g steel balls were put into a steel vial. Milling was performed under argon gas atmosphere with a rotational speed of 400 rpm. The milling process was stopped for 15 minutes after every 30 minutes of the work to prevent the temperature rise inside the vial. Some powders were taken out the vial within 8, 16, 24, and 32 hours of milling to analyze the phase transformation at various milling times.

In order to consalidation of the milled powders, the powders were pressed into a cylindrical steel mold with a load of 300 MPa. It should be noted that the dimensions of the produced billet were 30 mm in the length and the diameter of 27 mm. Then, the pressed samples were subjected to sintering process at a temperature of 800 °C for 30 min under the argon gas atmosphere.

In this study, X-ray diffraction analysis (XRD, D8 advance Bruker system, CuKα radiation) was performed to identify the phases during the MA. Also, the crystallite size and the lattice strain was measured by Williamson-Hall formula. The microstructure, morphology, and the particle size change at various stages of milling were studied by scanning electron microscopy (SEM, Camscan mv2300 system). The Archimedes method was used to measure the density of

the samples according to ASTM, C-373 standard [19]. Also, the mixtures law was used to calculate the theoretical density. The microhardness test was performed based on Vickers hardness by Coopa mh1 microhardness tester according to the standard of ASTM, E 384-99. The microhardness test was done at the load of 200 g for the loading time of 15 s.

3. RESULTS AND DISCUSSION

The X-ray diffraction patterns of the as-milled Zr-Cr powders and the milled powders are shown in Figure 1 to identify the phase evolution at milling times of 8, 16, 24, and 32 h. The Zr peaks were moved to the lower angles after 8 h of milling. The peak height of the elements is significantly reduced as compared with the initial powders and some peaks related to Zr and Cr were removed at 8 h. In addition, the width of the peaks was increased at that time.

The transition of Zr diffraction peaks to the lower angles indicated the dissolution of Cr in the Zr lattice. Factually, the dissolution of the Cr atoms with an atomic radius less than the atomic radius of the Zr atoms caused to solute the Cr atoms in the Zr lattice through two substitution and interstitial ways [20]. This matter led to apply the severe strain into Zr lattice, and so, the Zr lattice parameter was increased. Finally, the Zr peaks moved to the lower angles as the Zr lattice parameter was increased. It should be noted that the dissolution of the Cr atoms within Zr lattice in two forms of substitution and interstitial is owing to the high difference in the atomic radius of Zr and Cr.

Also, the Zr lattice parameter was calculated using Bragg's law [21]. Figure 2 is depicted the values of the lattice parameter versus milling time. The Zr lattice parameter was significantly increased up to 24 h of milling, but after 32 h, there was no noticeably change in the Zr lattice parameter which indicated the Cr atoms were completely dissolved in the Zr lattice after 24 h. The dissolution of Cr in the Zr lattice led to form the Zr(Cr) supersaturated solid solution phase with hcp crystalline lattice.
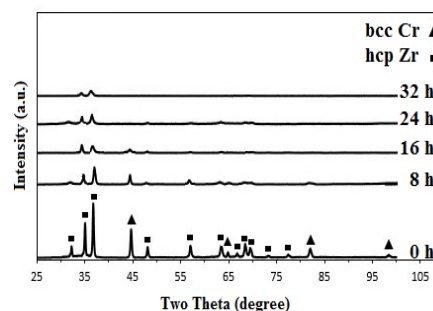
Figure 1. X-ray diffraction patterns of Zr-Cr powder mixtures versus milling time
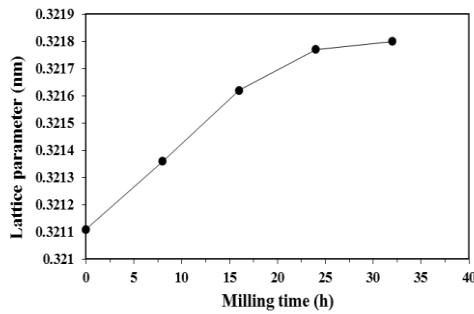
Figure 2. The change of Zr lattice parameter at different milling times

As mentioned, the atomic radius of Cr is lower than Zr atomic radius which led to solute Cr in Zr lattice both through an interstitial and a substitution way. This matter led to apply the severe strain into the Zr-rich phase and facilitated the amorphous phase formation [22]. So, the height of Zr peaks gradually decreased at the milling time of 8, and also, some peaks of Zr were eliminated at 16 h. On the other hands, the MA process was applied a severe plastic deformation to Zr lattice which led to work hardening of the powder particles. Therefore, a distortion in the Zr lattice was created which led to prepare the amorphous phase. The disappearance of Zr crystalline peaks is a sign of amorphous structure at the milling time of 16 h.

After 24 h of milling, the Zr peak at the angle of 32.5° was appeared. This appearance of Zr peak at 24 h was related to the local temperature rise in the milled powder which caused the nonequilibrium phases such as amorphous phase transformed to the more stable phases such as crystalline phase after 24 h of milling. The temperature of the milled powders could increase up to 300 °C at high milling times which led to occur the recovery and recrystallization phenomena [23]. In general, the recovery and recrystallization can significantly decrease the lattice strain due to the rearrangement of the dislocation, and the reduction of defect densities [24]. In fact, MA technique is considered to be a method for production of nonequilibrium phases but at milling, the local temperature enhancement due to the kinetic energy of the balls led to transformation of amorphous phase to more stable crystalline phase. In other words, the generation of the heat during milling increased the diffusivity of atoms and then, increased the tendency of formation the more stable phases. Principally, the change in the peak intensity depended on the plastic deformation in the recovery and recrystallization operation [25]. In other words, plastic deformation caused to decrease the peak intensity while, the recovery and recrystallization increased the peak intensity. Finally, the Zr peak at the angle of 32.5° was removed after 32 h of milling due to the severe deformation. The

reduction of the peak intensity continued up to 24 h and the Cr peaks were totally eliminated and also, the Zr peaks remains as the only crystalline phase. The peak widening continued as the milling time was increased, especially at 24 h of milling, which confirmed that many crystalline defects were created in the powders during the milling process. In other words, defects were the main reason of the enhancement of the peak width. The plot of the lattice strain and crystallite size versus milling time are shown in Figure 3. The lattice strain enhancement and crystallite size refinement were occurred as the milling time was enhanced, which confirmed that the responsible for the increase in the peak width was the crystallite size refinement and lattice strain enhancement. As observed in Figure 3, it is clear that the decrement rate of the crystallite size was decreased after 16 h of milling. Finally, after 32 h of milling, the crystallite size was found to be 19 nm, indicating that the MA process is a proper technique to produce the nanostructured powders.

When the crystallite size is nanometer scale, it is possible to dissolve the elements in each other and the formation of a solid solution in the alloy systems with a positive enthalpy [26]. In fact, the strain increased the distances between the atomic planes in the crystal lattice [24], which ultimately led to increase the diffusion of Cr in the Zr lattice. Finally, Zr(Cr) supersaturated solid solution was produced after 24 h.

However, this study indicated that the mechanical alloying of powders can enhance the solid solubility, and led to form the Zr(Cr) supersaturated solid solution phase. The high density of dislocation can significantly increase the solid solubility. In general, the effect of cold welding and fracture phenomena on the MA process led to apply the severe plastic deformation (SPD) on the powders. SPD increased the defect density, which led to facilitate the diffusion of the atoms. Finally, the alloying treatment was improved.

The morphology of the powders were studied by SEM images. Figure 4(a) shows the morphology of the primary powders of Zr and Cr. The particle size of the primary powders was approximately 5-50 μm, and the
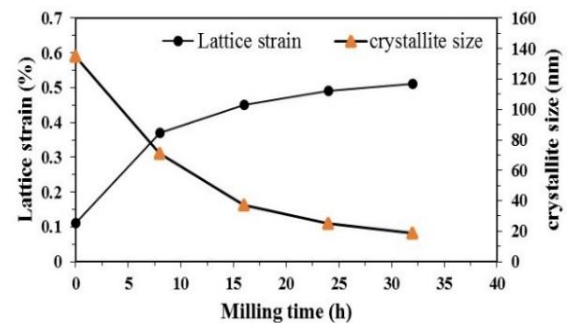
Figure 3. The change of lattice strain and Crystallite size of Zr element at various milling times

particle size distribution was irregular. The powder particles are very soft at the start of MA due to the low dislocation density, and high energy collisions was applied to the soft powders during the milling process. This high energy led to occur the plastic deformation in the powder particles, and the particles morphology became coarse-grained particles at 8 h which is indicated in Figure 4(b). In fact, the cold welding mechanism caused to stock the powder particles together. At 8 h, the particle size of the powder mixtures was about 75-175 µm with a heterogeneous distribution. In Figure 4(c), the mechanical bonding and cold welding among the Cr and Zr particles were happened after 16 h owing to the impact of the balls. It can be concluded that the particle size was increased as compared with the previous stage. They were randomly distributed with a size of about 1-80 µm. After 24 h, the work hardening was occurred due to the enhancement of the dislocation density which led to breakdown the particles. Therefore, the particle size was reduced to less than 30 µm which is shown in Figure 4(d).

(a)

(b)

(c)

(d)

(e)
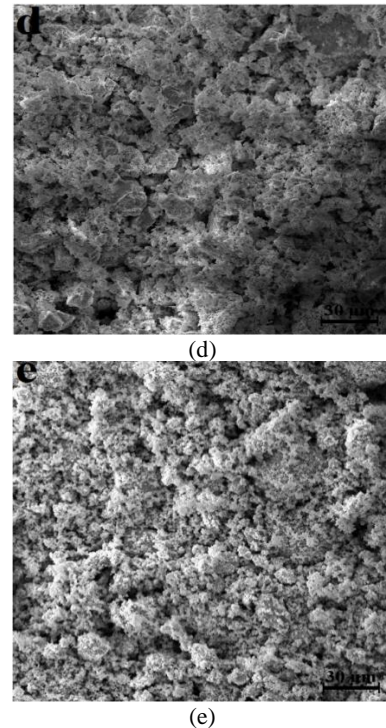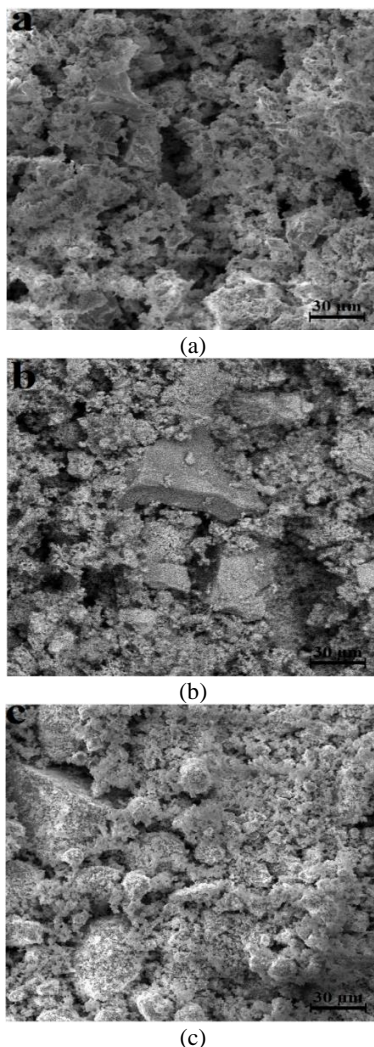
Figure 4. The SEM image of Zr(Cr) alloy at: (a) 0 h, (b) 8 h, (c) 16 h, (d) 24 h, and (e) 32 h of milling

In fact, the fracture of powder particles was the prodominant phenomenon. Finally, the particle size was reduced with an irregular distribution of the particle size. Of course, another factor that can contribute to the fragmentation of the particles was the dissolution of the elements, and work hardening owing to the formation of Zr(Cr) supersaturated solid solution phase [27]. The powder particles fracture continued after 32 h which is shown in Figure 4(e). At this time, the particle morphology was close to the spherical shape with a size of less than 20 µm which more regularly distributed as compared with the previous steps. In fact, the thickness of the particles was reduced owing to the severe deformation; thus, the diffusion distances were reduced. As a result, the decrement of the diffusion distances and the enhancement of the crystalline defects led to be more diffusion of the atoms which enhanced the solid solubility of the elements.

Figure 5 shows the results of the density measuring based on the Archimedes method. In this figure, the empirical values were compared with the theoretical values. As can be seen, the density of Zr-Cr alloy samples is close to the theoretical density (about 98% of the theoretical density). This can be attributed to the excessive deformation in the milling process. At the start of milling process, the density of the produced alloy was decreased which may be due to the agglomeration of powder particles at the beginning of the milling. Of course, the powder particle size can

greatly effect on the pressing and consolidation of the powder particles.

According to Figure 5, the density of Zr-Cr alloy was increased from 6.344 g/cm^3 at 8 h to 6.359 g/cm^3 after 24 h of milling. This is owing to the crystallite size refinement as well as the reduction in the powder particle size at longer milling times. Also, the density of the as-milled Zr-10 wt% Cr powders was increased from 6.349 g/cm^3 to 6.359 g/cm^3 after 24 h of milling. This is due to the reduction in the powder particle size, reduction in the crystallite size, complete diffusion of Cr into the Zr lattice, and the formation of Zr(Cr) phase during the milling process. Finally, the density of Zr-10 wt% Cr alloy reached to 6.362 g/cm^3 after 32 h of milling which is equal to 98% of the theoretical density.

To investigation of the mechanical properties of Zr(Cr) alloy, the microhardness test was performed and their results are depicted in Figure 6. The microhardness was enhanced as the milling time was enhanced. It should be noted that the microhardness of the primary powders was in the range of 118-129 Hv; which the lowest value was corresponding to Zr and the largest value was related to Cr. At 8 h, the microhardness was
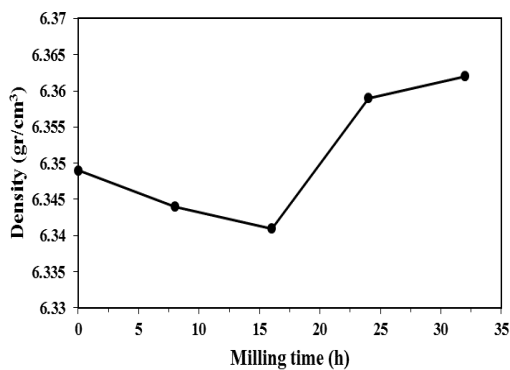
severely increased. This is due to the sharp decline in the crystallite size at the early stages of the milling. In fact, the primary powders are very soft and the work hardening of the powders due to the severe strain was responsible for the enhancement of the microhardness after 8 h.

After 16 h, the rate of the microhardness enhancement was decreased as compared with the previous stage. This trend continued up to 24 h. The microhardness value reached to 475 Hv after 24 h, indicating the microhardness was significantly increased. In fact, several factors including the crystallite size decrement, formation of the supersaturated solid solution, and the severe strain had a significant effect on the microhardness enhancement. The formation of the supersaturated solid solution of Zr(Cr) can improve the microhardness of Zr due to the solution hardening. In other words, the solution of Cr in Zr lattice through interstitial and substitution ways can prevent the movement of the dislocation which led to increase the microhardness of Zr-based alloy [24]. Eventually, after 32 h of milling, the microhardness reached to about 491 Hv, indicating that the microhardness didn't significantly change after 24 h and was almost stable. In fact, the Zr(Cr) supersaturated solid solution was formed at 24 h and no significant phase evolution was observed after the 32 h. However, homogenization of nanostructures and grain size reduction can effect on the microhardness.

Figure 5. Density of the Zr-Cr alloy versus milling times

4. CONCLUSION

In the present research, the effect of MA process and sintering on the behaviour of Zr and Cr powder mixtures in the immiscible Zr-Cr alloy system was investigated. As well-known, the solid solubility of Cr in Zr lattice is about 1% at the equilibrium state. The results revealed that MA led to enhance the solid solubility of Cr in Zr lattice. Finally, a nanostructure supersaturated solid solution of Zr(Cr) was formed. Therefore, the crystallite size of Zr was decreased to about 19 nm. The SEM images analysis indicated that at the beginning of MA, the cold welding was the dominant mechanism which led to agglomerate the powder particles, so that, the largest powder particle size reached to 80 μm after 16 h. the particle fracture dominated cold welding at 24 h of milling. After 32 h of milling, the particle size reached to 20 μm with a spherical shape and homogeneous distribution. The density of the Zr-10 wt% Cr alloy was close to 98% of the theoretical density. Also, the microhardness measurement revealed that MA could noticeably enhance the microhardness value of the Zr-10 wt% Cr alloy up to 491 Hv after 32 h.

Figure 6. Vickers microhardness value of the Zr(Cr) alloy versus milling time

5. REFERENCES

1. Zhang, X., Liu, S. G., Wang, S. H., Zhang, B., Zhang, X. Y., Ma, M. Z. and Liu, R. P., "Dynamic precipitation-induced simultaneous enhancement of the strength and plasticity of hot-rolled Zr–9Al alloy", *Journal of Alloys and Compounds*, Vol. 829, (2020), 154577. DOI: https://doi.org/10.1016/j.jallcom.2020.154577

2. Gault, B., Felfer, P. J., Ivermark, M., Bergqvist, H., Cairney, J. M. and Ringer, S. P., "Atom probe microscopy characterization of as quenched Zr-0.8 wt% Fe and Zr-0.15 wt% Cr binary alloys", *Materials Letters*, Vol. 91, (2013), 63-66. DOI: https://doi.org/10.1016/j.matlet.2012.09.059

3. Kuprin, A. S., Belous, V. A., Voyevodin, V. N., Bryk, V. V., Vasilenko, R. L., Ovcharenko, V. D., Reshetnyak, E. N., Tolmachova, G. N. and Vyugov, P. N., "Vacuum-arc chromium-based coatings for protection of zirconium alloys from the high-temperature oxidation in air", *Journal of Nuclear Materials*, Vol. 465, (2015), 400-406. DOI: https://doi.org/10.1016/j.jnucmat.2015.06.016

4. Ryabchikov, A. I., Kashkarov, E. B., Shevelev, A. E. and Syrtanov, M. S., "High-intensity chromium ion implantation into Zr-1Nb alloy", *Surface and Coatings Technology*, Vol. 383, (2020), 125272. DOI: https://doi.org/10.1016/j.surfcoat.2019.125272

5. Huang, M., Li, Y., Ran, G., Yang, Z. and Wang, P., "Cr-coated Zr-4 alloy prepared by electroplating and it's in situ He^+ irradiation behavior", *Journal of Nuclear Materials*, Vol. 538, (2020), 152240. DOI: https://doi.org/10.1016/j.jnucmat.2020.152240

6. Chen, K., Zeng, L., Li, Z., Chai, L., Wang, Y., Chen, L.Y. and Yu, H., "Effects of laser surface alloying with Cr on microstructure and hardness of commercial purity Zr", *Journal of Alloys and Compounds*, Vol. 784, (2019), 1106-1112. DOI: https://doi.org/10.1016/j.jallcom.2019.01.097

7. Prosviryakov, A. S., Bazlov, A. I. and Loginova, I. S., "Effect of Cu addition on microstructural evolution and hardening of mechanically alloyed Al−Ti−O in-situ composite", *Transactions of Nonferrous Metals Society of China*, Vol. 30, No. 5, (2020), 1135-1147. DOI: https://doi.org/10.1016/S1003-6326(20)65284-0

8. Akbari, G. H. and Taghian, M., "Behavior of Cu-Cr Powder Mixtures During Mechanical Alloying", *International Journal of Engineering*, Transactions B: Applications, Vol. 23, No. 1, (2010), 69-76. DOI: 10.5829/IJE.2010.23.01B.05

9. Mirvakili, S. A., Zakeri, M. and Yazdani Rad, R., "Effect of Chromium Content on Formation of $(Mo_{1-x}Cr_x)Si_2$ Nanocomposite Powders via Mechanical Alloying", *International Journal of Engineering*, Transactions C: Aspects, Vol. 25, No. 2, (2012), 99-104. DOI: 10.5829/IJE.2012.25.02C.02

10. Suryanarayana, C. and Al-Joubori A. A., "Effect of initial composition on phase selection in Ni-Si powder blends processed by mechanical alloying", *Materials and Manufacturing Processes*, Vol. 33, No. 8, (2018), 840-848. DOI: 10.1080/10426914.2017.1401714

11. Akbari, G. H. and Khajesarvi, A., "Effect of Mo Addition on Nanostructured $Ni_{50}Al_{50}$ Intermetallic Compound Synthesized by Mechanical Alloying", *International Journal of Engineering*, Transactions C: Aspects, Vol. 28, No. 9, (2015), 1328-1335. DOI: 10.5829/IJE.2015.28.09C.10

12. Verdian, M. M., "Fabrication of supersaturated NiTi(Al) alloys by mechanical alloying", *Materials and Manufacturing Processes*, Vol. 25, No. 12, (2010), 1437-1439. DOI: https://doi.org/10.1080/10426914.2010.501093

13. Azazari khosroshahi, R., Abbasi Nargesi, F. and parvini ahmadi, N., "Synthesis of Nanostructure Ti-45Al-5Cr Alloy by Mechanical Alloying and Study the Effect of Cr Addition on Microstructure of TiAl Alloy", *International Journal of Engineering, Transactions A: Basics*, Vol. 24, No. 2, (2011), 123-130. DOI: 10.5829/IJE.2011.24.02C.03

14. Rahaei, M. B., Yazdani-Rad, R. and Kazemzadeh, A., "Synthesis and Characterization of Nanocrystalline Ni_3Al Intermetallic during Mechanical Alloying Process", *International Journal of Engineering, Transactions C: Aspects*, Vol. 25, No. 2, (2012), 89-98. DOI: 10.5829/IJE.2012.25.02C.01

15. Kristl, M., Ban, I. and Gyergyek, S., "Preparation of Nanosized Copper and Cadmium Chalcogenides by Mechanochemical Synthesis", *Materials and Manufacturing Processes*, Vol. 28, No. 9, (2013), 1009-1013. DOI: https://doi.org/10.1080/10426914.2013.811736

16. Zhang, X., Li, Y., He, X., Sun, Y., Pang, S., Su, G., Liu, X., and Yang, Z., "Influence of Cr addition on microstructure and mechanical properties of Zr-based alloys corresponding to Zr-C-Cr system", *Journal of Alloys and Compounds*, Vol. 640, (2015), 240-245. DOI: https://doi.org/10.1016/j.jallcom.2015.03.240

17. Ali, F., Mehmood, M., Qasim, A. M., Ahmada, J., Rehman, N., Iqbal, M., and Qureshi, A. H., "Comparative study of the structure and corrosion behavior of Zr-20%Cr and Zr-20%Ti alloy films deposited by multi-arc ion plating technique", *Thin Solid Films*, Vol. 564, (2014), 277-283. DOI: https://doi.org/10.1016/j.tsf.2014.05.041

18. Massalski, T. B., Okamoto, H., Subramanian, P.R. and Kacprzak, L., Binary Alloy Phase Diagrams, ASM International, Ohio: Materials Park, 1990.

19. Kumar, A. A., Patton, M. R., Hennek, J. W., Lee, S. Y. R., Alesio-Spina, G. D., Yang, X., Kanter, J., Shevkoplyas, S. S., Brugnara, C. and Whitesides, G. M., "Density-based separation in multiphase systems provides a simple method to identify sickle cell disease", *Proceedings of the National Academy of Sciences*, Vol. 111, No. 5, (2014), 14864-14869. DOI: https://doi.org/10.1073/pnas.1414739111

20. Burr, P. A., Wenman, M. R., Gault, B., Moody, M. P., Ivermark, M., Rushton, M. J. D., Preuss, M., Edwards, L. and Grimes, R. W., "From solid solution to cluster formation of Fe and Cr in α-Zr", *Journal of Nuclear Materials*, Vol. 467, No. 1, (2015), 320-331. DOI: https://doi.org/10.1016/j.jnucmat.2015.10.001

21. Cullity, B. D. and Stock, S. R., Elements of X-ray Diffraction, New York: Pearson, 2001.

22. Nowroozi, M. A., and Shokrollahi, H., "Magnetic and structural properties of amorphous/nanocrystalline $Fe_{42}Ni_{28}Zr_8Ta_2B_{10}C_{10}$ soft magnetic alloy produced by mechanical alloying", *Advanced Powder Technology*, Vol. 24, No. 6, (2013), 1100-1108. DOI: https://doi.org/10.1016/j.apt.2013.03.016

23. Suryanarayana, C., "Mechanical alloying and milling", *Progress Materials Science*, Vol. 46, No. 1-2, (2001), 1-184. DOI: https://doi.org/10.1016/S0079-6425(99)00010-9

24. Dieter, G.E., mechanical metallurgy, New York: McGraw-Hill Book Co., 1986.

28. Lou, T., Fan, G., Ding, B., and Hu, Z., "The synthesis of $NbSi_2$ by mechanical alloying". *Journal of Materials Research*, Vol. 12, No. 5, (1997), 1172-1175. DOI: https://doi.org/10.1557/JMR.1997.0162

25. Costa, M.B., Mateus, R., Guedes, M. and Ferro, A. C., "Mechanical alloying in the Li-Sn system", *Materials Letters: X*, Vol. 6, No. 1, (2020), 100045. DOI: https://doi.org/10.1016/j.mlblux.2020.100045

26. Annan, K. A., Daswa, P., Motumbo, K. and Siyasiya, C. W., "Influence of milling parameters on the structural and phase

formation in Ti-20%Al alloy through mechanical milling", ***Materials Today***, (2020). DOI: https://doi.org/10.1016/j.matpr.2020.04.524

27. Zhao, C., Lu, H., Wang, H., Tang, F., Nie, H., Hou, C., Liu, X., Song, X. and Nie, Z., "Solid-solution hardening of WC by

rhenium", ***Journal of the European Ceramic Society***, Vol. 40, No. 2, (2020), 333-340. DOI: https://doi.org/10.1016/j.jeurceramsoc.2019.09.050

Persian Abstract

چکیده

هدف از پژوهش حاضر، تولید آلیاژ پایه Zr به عنوان روکش سوخت هسته‌ای با استفاده از فرآیند آلیاژسازی مکانیکی (MA) و تفجوشی است. بدین منظور، پودرهای Zr و Cr برای تولید آلیاژ دیرگداز و سخت Zr-10 wt% Cr به صورت مکانیکی آلیاژسازی شدند و سپس، مخلوط پودر بوسیله پرس و سینتر در دمای ۸۰۰ °C به مدت ۳۰ دقیقه فشرده شد. تغییر فاز، تغییرات ریزساختار، ریزسختی و چگالی آلیاژهای حاصل با استفاده از پراش اشعه ایکس (XRD)، میکروسکوپ الکترونی روبشی (SEM)، اندازه‌گیری میکروسختی و روش ارشمیدوس مورد بررسی قرار گرفت. نتایج نشان داد که MA باعث افزایش حلالیت پودرهای غیرقابل امتزاج Cr و Zr در حالت جامد می‌شود، به طوری که اتم‌های Cr پس از ۲۴ ساعت آسیاکاری به طور کامل در شبکه Zr حل شدند و محلول جامد نانوساختار Zr(Cr) با مقدار سختی 491 Hv حاصل شد. همچنین، نتایج اندازه‌گیری چگالی نشان داد که چگالی حاصل نزدیک به ۹۸٪ چگالی نظری است.